THE JOURNAL OF BIOLOGICAL CHEMISTRY
Vol. 276, No. 16, Issue of April 20, pp. 13169–13177, 2001
Printed in U.S.A.

Homo- and Heterooligomeric SNARE Complexes Studied by Site-directed Spin Labeling*

Received for publication, November 26, 2000, and in revised form, January 17, 2000
Published, JBC Papers in Press, January 19, 2001, DOI 10.1074/jbc.M010653200

Martin Margittai‡, Dirk Fasshauer‡, Stefan Pabst‡, Reinhard Jahn‡§, and Ralf Langen¶

From the ‡Department of Neurobiology, Max-Planck-Institute for Biophysical Chemistry, 37077 Göttingen, Germany and the ¶Department of Biochemistry and Molecular Biology, Institute for Genetic Medicine and Neurogenetic Institute, University of Southern California, Los Angeles, California 90033

SNARE (soluble NSF acceptor protein receptor) proteins are thought to mediate membrane fusion by assembling into heterooligomeric complexes that connect the fusing membranes and initiate the fusion reaction. Here we used site-directed spin labeling to map conformational changes that occur upon homo- and heterooligomeric complex formation of neuronal SNARE proteins. We found that the soluble domains of synaptobrevin, SNAP-25, and syntaxin 1 are unstructured. At higher concentrations, the SNARE motif of syntaxin 1 forms homooligomeric helical bundles with at least some of the α-helices aligned in parallel. In the assembled SNARE complex, mapping of thirty side chain positions yielded spectra which are in good agreement with the recently published crystal structure. The loop region of SNAP-25 that connects the two SNARE motifs is largely unstructured. C-terminal truncation of synaptobrevin resulted in complexes that are completely folded N-terminal of the truncation but become unstructured at the C-terminal end. The binary complex of syntaxin and SNAP-25 consists of a parallel four helix-bundle with properties resembling that of the ternary complex.

SNARE[1] proteins represent a superfamily of small and mostly membrane-bound proteins that mediate intracellular membrane fusion in eukaryotic cells (1–5). Both the structure and the molecular mechanism of SNAREs in membrane fusion have been subject of intense investigations. The SNAREs functioning in neuronal exocytosis have served as paradigms for the other members of the protein family. They include the plasma membrane proteins syntaxin 1, SNAP-25 (acronym for synaptosome-associated protein of 25 kDa), and the synaptic vesicle protein synaptobrevin (also referred to as VAMP). These proteins assemble spontaneously into a stable ternary complex that can be disassembled by the ATPase chaperone NSF (*N*-ethylmaleimide-sensitive factor) in conjunction with SNAP proteins as cofactors (SNAP stands for soluble NSF attachment protein, no relation to SNAP-25) (6, 7). It is currently thought that assembly of the SNARE proteins ties the fusing membranes together and thus initiates the fusion reaction (8).

As a common feature, all SNAREs contain a homologous stretch of 60 amino acids referred to as the SNARE motif (9–11). Syntaxin 1 and synaptobrevin each contain a single SNARE motif directly adjacent to their C-terminal transmembrane domain. SNAP-25 does not possess a transmembrane domain. It is composed of two SNARE motifs, one at the C- and one at the N-terminal end. The motifs are connected by a loop containing palmitoylated cysteines. Limited proteolysis of ternary complexes as well as site-directed mutagenesis revealed that the SNARE motifs form a tight complex (also referred to as core complex) whereas other regions of the molecules do not participate in complex formation (12–21). The crystal structure of the neuronal core complex represents an elongated and twisted bundle of four α-helices that are aligned in parallel with each corresponding to one SNARE motif of the neuronal SNAREs (22). The center of the bundle contains 16 layers of interacting and mostly hydrophobic side chains that are stacked perpendicular to the axis of the helix bundle. In the middle of the bundle, an unusual "0" layer was found that is composed of three Gln residues (contributed by syntaxin and SNAP-25) and one Arg residue (contributed by synaptobrevin). These residues are highly conserved throughout the entire SNARE superfamily, leading to their classification into Q-SNAREs and R-SNAREs, respectively (23).

Whereas synaptobrevin and SNAP-25 do not possess additional structured regions, the N-terminal region of syntaxin is represented by an independently folded domain. Both NMR spectroscopy and crystallography of the isolated N-terminal domain showed an antiparallel bundle of three α-helices that is stabilized both by hydrophobic and hydrophilic interactions (24–26). When syntaxin is not complexed with its SNARE partners, the N-terminal domain is bound to the N-terminal part of the SNARE motif (15, 27–28). Crystallization of syntaxin in complex with munc-18/n-sec1 revealed that in the closed conformation the SNARE motif of syntaxin has a different structure from that in the core complex (26). Only the N-terminal portion is α-helical, which is followed by a few short turns and helices, whereas the C-terminal end is unstructured.

Assembly of the core complex is associated with major conformational changes (29). CD and NMR spectroscopy showed that monomeric synaptobrevin and monomeric SNAP-25 exhibit no significant secondary structure (29–31). Recently, the structure of synaptobrevin in complex with botulinum neurotoxin B, a bacterial protease selective for the protein, has been determined by x-ray crystallography (32). The new structure does not contain identifiable secondary structure elements and is thus very different from the conformation in the core complex.

* This work was supported by a grant from the VW-Foundation (to R. J.) and by the James H. Zumberge Faculty Research Innovation Fund (to R. L.). The costs of publication of this article were defrayed in part by the payment of page charges. This article must therefore be hereby marked "*advertisement*" in accordance with 18 U.S.C. Section 1734 solely to indicate this fact.

§ To whom correspondence should be addressed: Dept. of Neurobiology, Max-Planck-Institute for Biophysical Chemistry, Am Fassberg 11, Göttingen 37077, Germany. Tel.: 49-551-201-1635; Fax: 49-551-201-1639; E-mail: rjahn@gwdg.de.

[1] The abbreviations used are: SNARE, soluble NSF acceptor protein receptor; SNAP-25, synaptosome-associated protein of 25 kDa; NSF, *N*-ethylmaleimide-sensitive factor; EPR, electron paramagnetic resonance; CD, circular dichroism; DTT, dithiothreitol; PAGE, polyacrylamide gel electrophoresis.

Because assembly of SNARE complexes plays a crucial role in fusion, it is essential to understand the details of the assembly reaction, including the structure of intermediate stages. For instance, it is unknown whether all three proteins assemble simultaneously or whether binary complexes must precede the formation of the ternary complex. Syntaxin and SNAP-25 can form binary complexes consisting of two syntaxins and one SNAP-25 molecule. Because one of the syntaxins can be replaced by synaptobrevin, binary complexes may serve as a precursor in membrane fusion (29). Furthermore, it is currently thought that core complex formation is initiated at the N-terminal end of the SNARE motifs, but it is not known whether a step-by-step assembly of the helix bundle is possible. Such a reaction pathway would require that intermediates exist in which part of the complex is helical, whereas the remainder of the proteins is unstructured. Loosely assembled intermediates have been postulated (33), but so far there is no direct evidence for the existence of partially assembled complexes.

In the present study, we have investigated the structure of monomeric as well as homo- and heterooligomeric complexes of neuronal SNARE proteins using site-directed spin labeling in combination with other biophysical techniques. Typically, site-directed spin labeling involves labeling of single Cys residues with a nitroxide reagent resulting in a disulfide-linked side chain. The electron paramagnetic resonance (EPR) spectrum of the protein-attached spin label depends on its local environment and can be used to identify a given site as a loop, exposed, buried, or tertiary contact (for review see Refs. 34–37). The relationship between EPR spectra of attached spin label and protein structure has been well-characterized (38), including a recent crystal structure analysis of spin-labeled T4 lysozyme derivatives (39). Furthermore, site-specific introduction of two paramagnetic centers in a protein provides a means of estimating inter-residue distances through magnetic interactions between the centers (34, 40–41). Thus, site-directed spin labeling can provide information on the location and type of secondary structural elements, a map of tertiary contact surfaces, and specific inter-residue distances. Collectively, this information can provide sufficient constraints to model a protein at the level of the backbone fold. Using such an approach, the overall topology of the neuronal SNARE complex has been accurately determined (42), and in addition, partial structural determinations have been performed for a number of soluble and membrane proteins (for review see Refs. 34–37). Here we have used site-directed spin labeling in combination with circular dichroism and absorption spectroscopy to obtain structural information about monomeric and oligomeric SNARE proteins. Our results reveal that SNAREs are highly adaptable molecules that can switch from random coil to α-helical conformations, offering new insights into the pathways by which these proteins assemble and disassemble.

EXPERIMENTAL PROCEDURES

Materials—Spin-label (1-oxy-2,2,5,5-tetramethylpyrrolinyl-3-methyl)methanthiosulfonate) was a kind gift from Dr. Kalman Hideg (University of Pecs, Hungary). Alexa594-maleimide was purchased from Molecular Probes. Cysteine-free protein fragments were derived from plasmids encoding SNAP-25A-(1–206) (all four cysteines substituted by serines) (43), syntaxin 1A-(180–262) (22), and synaptobrevin 2-(1–96) (21).

Plasmid Construction—Single cysteine substitutions were introduced by primer-mediated mutagenesis (44) using the *Pfu* DNA polymerase. In the case of syntaxin 1A, fragments were generated that encompassed amino acids 183–262. For synaptobrevin and SNAP-25 fragment sizes were as above. The following single mutations were introduced into syntaxin: L192C, T197C, N207C, E224C, S225C, Q226C, E238C, H239C, A240C, V248C, S249C, D250C, Y257C, Q258C, S259C, into synaptobrevin: S28C, S61C, T79C, and into SNAP-25: Q20C, L33C, L47C, V48C, M49C, H66C, K79C, S84C, S92C, A100C, S115C, S130C, V153C, G155C, R161C, T173C, T200C. While all synaptobrevin and syntaxin constructs were subcloned into pET28a (Novagen) via the *Nde*I/*Xho*I restriction site, SNAP-25 mutants were inserted into the *Nhe*I/*Xho*I site. Truncated synaptobrevin (residues 1–76) and syntaxin 1A (residues 180–253) constructs were both produced by conventional polymerase chain reaction and subcloned into pet15a via *Nde*I/*Xho*I restriction sites. Correctness of the DNA sequences was confirmed by DNA sequencing.

Protein Expression and Purification—Proteins were expressed according to standard protocols (43). The N-terminal His_6-tags served to affinity purify the proteins using nickel-nitrilotriacetic acid-agarose (Qiagen). After elution from the columns (elution buffer: 400 mM imidazole, 250 mM NaCl, 25 mM Tris, pH 7.4), the tags were cleaved off by thrombin. Cleavage occurred overnight during concomitant dialysis (50 mM NaCl, 20 mM Tris, pH 7.4, 1 mM DTT). The vector-derived residues GSH (syntaxin, synaptobrevin) and GSHMAS (SNAP-25) remained attached to the N termini of the fragments. Subsequently, the proteins were purified using MonoQ (syntaxin and SNAP-25) or MonoS columns (synaptobrevin) on an Äkta system (Amersham Pharmacia Biotech). All proteins were analyzed by SDS-PAGE and determined to be at least 95% pure. Binary and ternary complexes were formed overnight with one of the SNARE proteins containing a single cysteine substitution. The nonsubstituted mutants were used in 1.4- to 2-fold molar excess over the single cysteine proteins. Complex formation was verified by nondenaturing PAGE (binary complexes) or SDS-PAGE (ternary complexes). All single cysteine mutants were found to be quantitatively bound into complexes. Excess protein was separated from complexes by anion exchange chromatography (MonoQ, Amersham Pharmacia Biotech).

Truncated complexes were formed using a 2-fold molar excess of the purified cysteine-free SNAREs over the single cysteine mutant. Complexes were allowed to form overnight on ice and were not further purified.

Spin Labeling and EPR Measurements—DTT was removed by size-exclusion chromatography using PD-10 columns (Amersham Pharmacia Biotech) (equilibration buffer: 20 mM HEPES, pH 7.4, 400 mM NaCl). Immediately thereafter a 10- to 20-fold excess of the cysteine specific spin label (1-oxy-2,2,5,5-tetramethylpyrrolinyl-3-methyl)methanthiosulfonate) was added and allowed to react for at least 90 min at 25 °C. In the case of buried residues, incubations took place for up to 5 h. Unreacted label was removed by size-exclusion chromatography (PD-10 columns). Proteins were concentrated in Microcons (Amicon) and subsequently diluted with sucrose (final buffer: 30% sucrose (w/w), 240 mM NaCl, 20 mM Tris, pH 7.4). The protein concentrations ranged from 50 to 100 μM. 30% sucrose was used to reduce the rotational correlation time for the monomeric or oligomeric proteins.

EPR spectra were obtained using a Bruker EMX spectrometer. All spectra were recorded at 2-mW incident microwave power using a field modulation of 1.5 G at 100 kHz. Unless noted otherwise, the spectral breadth was 100 G. For the determination of spin-spin interactions of syntaxins in binary complexes labeled and unlabeled syntaxin (1:1 molar ratio) were combined and subsequently mixed with an equal molar amount of SNAP-25 (due to the 2 (syntaxin):1 (SNAP-25) stoichiometry of the binary complex SNAP-25 was used in 100% excess). Complex formation occurred overnight on ice.

Other Spectroscopic Techniques—Binary complexes containing syntaxins with single cysteine substitutions in position 197 were labeled with a 10-fold molar excess of Alexa594-maleimide. Incubations were carried out for 3 h on ice. The reactions were stopped with excess DTT. Noncoupled label was removed by gel filtration (PD-10). The sample was dialyzed overnight against phosphate-buffered saline, 1 mM DTT. For ternary complex formation, 1.32 μM labeled binary complex was reacted for 1 h with 13.2 μM synaptobrevin. Absorption spectra were recorded of either binary complex alone, or after adding synaptobrevin, using a Shimadzu (UV-2401 PC) spectrophotometer.

Multiangle laser light scattering and circular dichroism measurements were performed as described previously (43).

RESULTS

As starting point for the experiments we used recombinant versions of the cytoplasmic domain of synaptobrevin 2 (residues 1–96), the SNARE motif of syntaxin 1a (residues 183–262), and a full-length version of SNAP-25 in which the four cysteines of the linker region were replaced with serines. Substitutions of single amino acid residues with cysteines were then performed by site-directed mutagenesis. Using the crystal

structure of the core complex as a guide, residues were chosen that cover the full-length of the helix bundle and that represent buried, tertiary contact, and helix surface sites. Binary and ternary complexes were formed by appropriate monomer combination (30). All proteins and complexes were purified to more than 95% purity by a combination of affinity and ion exchange chromatography (43) and labeled with the cysteine-specific spin label (1-oxy-2,2,5,5-tetramethylpyrrolinyl-3-methyl)methanthiosulfonate; Fig. 1).

Individual SNAREs and SNARE Core Complexes in Solution—In the first set of experiments, a total of 12 sites were labeled in the two SNARE motifs of SNAP-25. Spectra were recorded from each of the SNAP-25 variants either as monomers or in core complexes with unlabeled synaptobrevin 2 and syntaxin 1a. Overlays of each of the corresponding spectra are shown in Fig. 2. From a detailed analysis of these spectra the following conclusions can be drawn. First, the spectra of all monomers were very similar to each other. Each spectrum was dominated by sharp and narrowly spaced peaks (central line width typically 2.5 G or less) that reflect a high degree of motion. Such high mobility is characteristic for unstructured regions (34–36, 38). Second, profound spectral differences were observed in the core complex at each site, indicating the formation of an ordered structure. In general, the characteristic

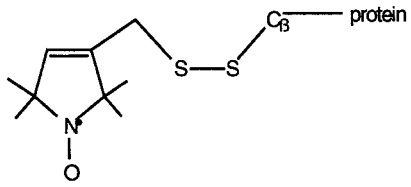

FIG. 1. **Chemical structure of the spin-label (1-oxy-2,2,5,5-tetramethylpyrrolinyl-3-methyl)methanthiosulfonate) attached to a cysteine side chain.**

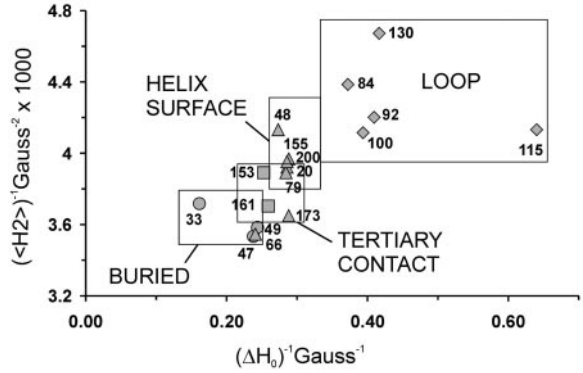

FIG. 3. **Plot of reciprocal second moment (⟨H2⟩) *versus* reciprocal central line width (ΔH_o) calculated from the EPR spectra of ternary complexes containing labeled SNAP-25 variants as shown in Fig. 2.** Positions that in the crystal structure are in loop regions are indicated by *diamonds*, positions on helix surfaces by *triangles*, positions in tertiary contact by *squares*, and those being buried, *i.e.* pointing toward the interior of the helix bundle, by *circles*.

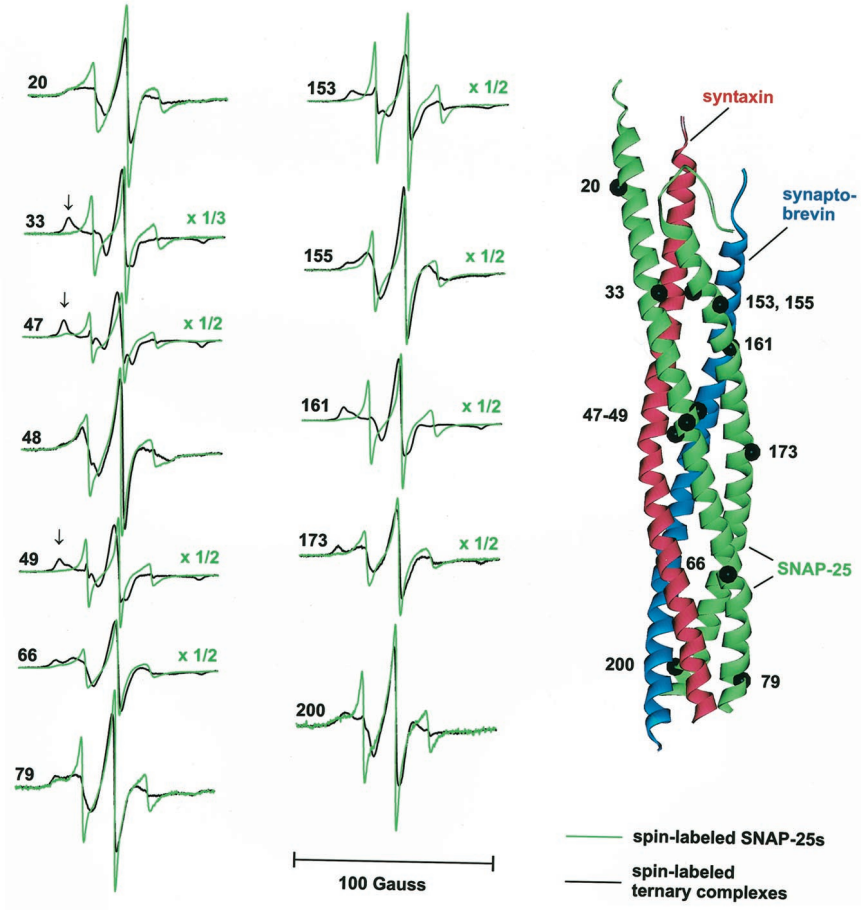

FIG. 2. **EPR spectra of spin-labeled SNAP-25 variants in isolation or as part of ternary SNARE complexes.** The positions in which spin labels were introduced are mapped on the crystal structure of the ternary complex (*right*). For each labeling position, spectra were recorded either in isolation (*green*) or after formation and purification of ternary complexes with synaptobrevin and the SNARE motif of syntaxin (*black*). To facilitate comparison of the spectra, the amplitudes of the indicated spectra were multiplied with either 1/2 or 1/3. *Arrows* indicate outer peaks characteristic for immobile side chains. Unless indicated otherwise, the scan width of these and all subsequent spectra is 100 G.

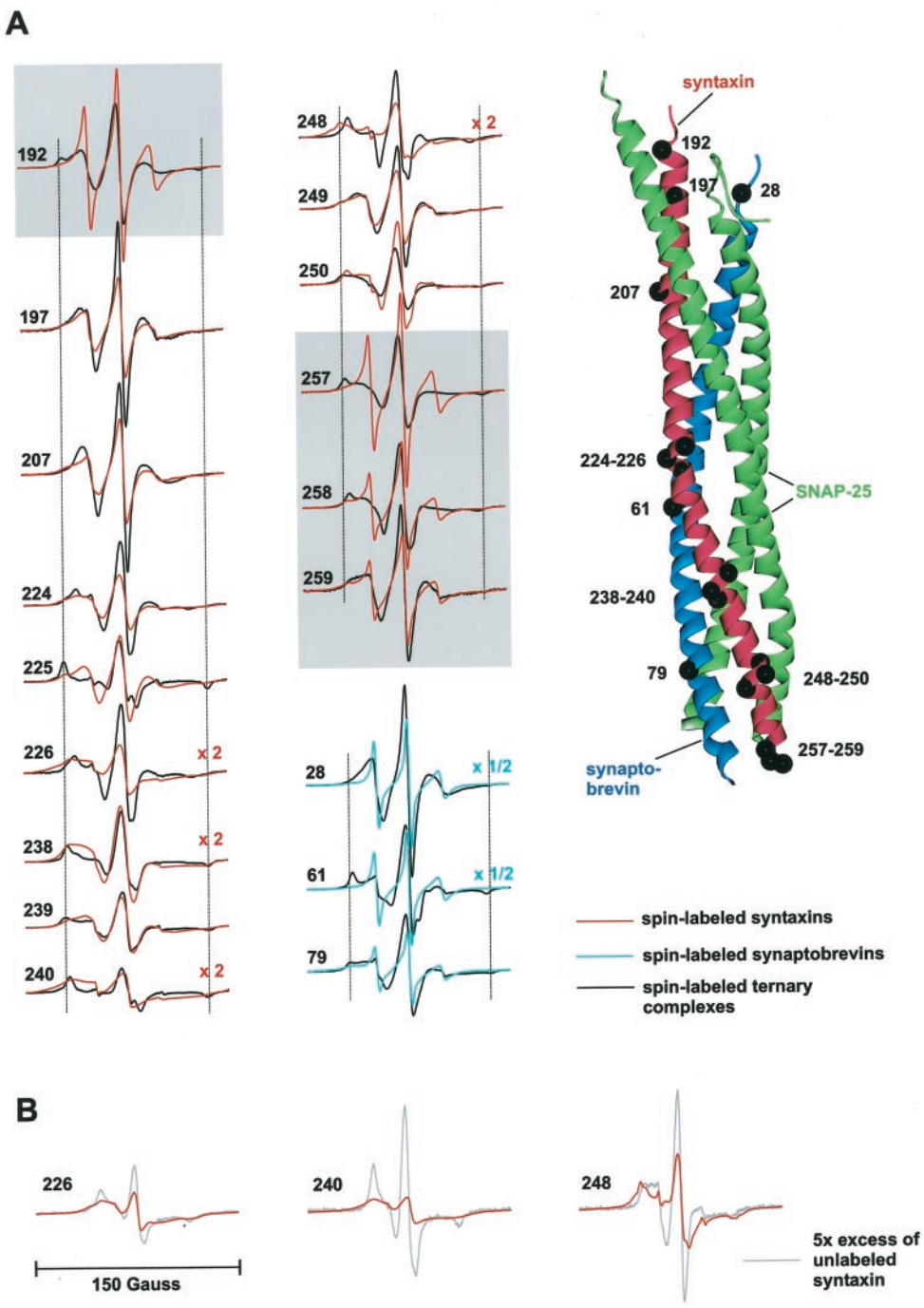

FIG. 4. **EPR spectra of spin-labeled syntaxin (SNARE motifs) and synaptobrevin variants in isolation or in ternary complexes.** *A*, comparison of sets of spectra obtained from spin-labeled syntaxin and synaptobrevin variants. Spectra were recorded either in isolation (*red*, syntaxin; *blue*, synaptobrevin) or after formation and purification of ternary complexes (*black*). To facilitate comparison, the amplitudes of some of the spectra were multiplied with the factors indicated. *Vertical lines* mark hyperfine extrema characteristic for immobilized spin label. Highly mobile spectra of syntaxin variants in isolation (*red*) are indicated by *shaded areas*. *B*, spin-spin coupling in isolated SNARE motifs of syntaxin. Syntaxin variants spin labeled at positions 226, 240, and 248 were diluted with unlabeled syntaxin (~5-fold molar excess). Spectra of undiluted syntaxins are depicted in *red*, spectra of diluted syntaxins in *black* (*dotted*). The scan width is 150 G. In all cases, addition of unlabeled syntaxin reduced spectral width and increased the amplitudes

features of the individual spectra from the core complex are in excellent agreement with the crystal structure (22). For example, the lowest mobility is seen at positions 33, 47, and 49, *i.e.* sites that are buried in the crystal structure. Characteristic for immobile side chains are the strongly broadened lines and the increased separation between the outer peaks (see *arrows* in Fig. 2). In contrast, residues 20, 48, 79, 155, and 200 yielded spectra indicative of mobile side chains, although not as sharp as in the monomers (compare *green* and *black traces* in Fig. 2). Such spectra are typically seen at helix surface sites (38), again in good agreement with their location in the crystal structure. All other sites exhibited intermediate mobility and can be classified as tertiary contact sites (except for residue 173, which is unusually immobile for a helix surface site).

Furthermore, we determined the inverse second moment and the inverse central line width, for each of the SNAP-25 core complex spectra (Fig. 3). It was first shown for spin-labeled T4 lysozyme that the combined use of these mobility parameters

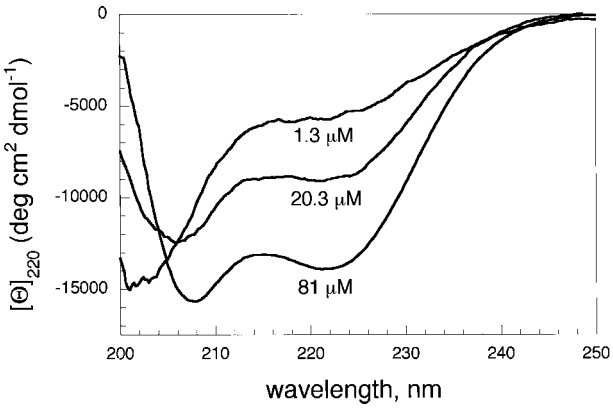

FIG. 5. **Progressive decrease in α-helicity upon dilution of syntaxin SNARE motifs.** CD spectra were recorded at three different protein concentrations (40 mM sodium phosphate buffer). Note that in this experiment a slightly longer fragment of syntaxin was used (residues 180–262 instead of 183–262).

TABLE I
Comparison of the molecular weights of various complexes determined by multiangle laser light scattering and the theoretical weights of monomers

Complex	Theoretical mass	Measured mass
	kDa	
Binary complex	49.3	54.1 ± 1.5
Ternary complex without SNAP-25 loop	41.2	79.3 ± 0.8
Ternary complex	44.4	88.8 ± 1.3
Ternary complex TeNT	41.8	46.5 ± 1.0
Ternary complex BoNT/C	43.3	43.3 ± 1.0

provides an effective means for distinguishing between loop, surface, tertiary contact, and buried sites (38). Reminiscent of the T4 lysozyme data, the respective sites in the core complex also cluster into different regions of the mobility plot in Fig. 3. These results further underscore the good agreement between the crystal structure and the site-directed spin labeling data.

Next, 15 different positions in the SNARE motif of syntaxin were individually labeled (Fig. 4*A*). Unlike synaptobrevin and SNAP-25, the free SNARE motif of syntaxin was previously reported to be at least partially α-helical (21). Furthermore, it is known to oligomerize (19, 21). Spectral analysis of the spin-labeled free proteins revealed that only the outermost N- and C-terminal positions (residue 192 at one end and residues 257, 258, and 259 at the other) are mobile, whereas all other positions suggest the formation of a folded structure (Fig. 4*A*). Generally, positions localized to the helix surface in the core complex also exhibited spectral characteristics of surface sites (residues 197, 207, 224, 225, 238, 239, 249, 250), suggesting that these residues again might be localized to the surface of a helix. For independent confirmation of syntaxin's secondary structure, we performed circular dichroism spectroscopy, which can be used at protein concentrations lower than required for EPR measurements. As shown in Fig. 5, the SNARE motif of syntaxin yielded a typical α-helical spectrum at 81 μM but became increasingly unstructured upon dilution. Together, these data show that the SNARE motif of syntaxin is unstructured and monomeric (as confirmed by multiangle laser light scattering, not shown) at concentrations below 2 μM and oligomerizes into helical bundles at increasing concentrations.

Interestingly, the spectra of all positions pointing inwards in the crystal structure of the core complex (residues 226, 240, 248) exhibited broadening beyond 100 G. Such broadening is a sign of strong spin-spin interactions which is observed only if the labeled positions are less than 15 Å apart (34). Indeed, when unlabeled syntaxin was added, sharper peaks and narrowing of the spectra was observed (Fig. 4*B*). Thus, corresponding residues of the individual helices in the oligomer must be in close proximity at each of these labeling positions, which can only be reconciled with a parallel alignment of the helices. In addition, the side chains pointing inward in the core structure also point inward in the syntaxin homooligomer, indicating that the overall alignment of the helices is similar. At all other sites significantly weaker or no coupling was observed.

Next, EPR spectra were recorded from core complexes containing the spin-labeled syntaxin derivatives (Fig. 4*A*, *black spectra*). Spectra from the N-terminal helix surface sites 192, 197, and 207 showed the characteristic features of helix surface sites. Also in good agreement with the crystal structure is the fact that inwardly pointing positions (226, 240, 248, and 257) exhibited highly immobile components.

The EPR spectra of C-terminal helix surface sites gave rise to uncharacteristically immobile components (residues 224, 225, 238, and 239) (Fig. 4*A*). These are best explained by surface contacts between several SNARE complexes. Such oligomer formation was previously reported (19, 21) (Table 1). Moreover, in the crystal structure three asymmetrically arranged complexes were found per unit cell that form contacts in the C-terminal region. To examine whether neighboring positions in the adjacent synaptobrevin helix are affected in a similar manner, we generated three spin-labeled derivatives of synaptobrevin. As shown in Fig. 4*A*, only the spectrum of the most N-terminal labeling position (residue 28) was typical for a helix surface localization, whereas immobile peaks were observed both at positions 61 and 79, with position 61 being more pronounced. In synaptobrevin monomers, all three positions were highly mobile, in agreement with the notion that free synaptobrevin is unstructured.

Interestingly, the spectrum of position 225 of syntaxin shows no mobile component, although this residue has no side-chain contacts in the crystal structure of one of the three complexes in the unit cell. A tertiary contact with the loop connecting the two SNARE motifs of SNAP-25 (which were removed for crystallization, see below) can be excluded, because removal of the loop did not change the spectrum (not shown). These findings suggest that the oligomeric interactions in solution may be somewhat different from that in the crystal.

The data described so far demonstrate that the structural features of the ternary complex in solution as determined by EPR spectroscopy are in good agreement with the crystal structure. The only exception relates to an oligomeric interaction between complexes that involves the C-terminal regions of all four helices and that is not matched by corresponding crystal contacts. Furthermore, the data confirm that the monomeric forms of synaptobrevin and SNAP-25 are unstructured over the entire length of the SNARE motif, whereas the SNARE motif of syntaxin forms oligomeric helical bundles at higher concentrations in which each helix appears to have an orientation with respect to surface exposure and buried residues that is similar to the ternary complex. Together with a previous report (42), these findings validate the spin labeling approach as a powerful tool for the study of SNARE structure and enabled us to determine features of the SNAREs for which structural information is not available.

Loop Region of SNAP-25—Previous data showed that the region of SNAP-25 connecting the two SNARE motifs is sensitive to proteases (19, 21), and it was therefore not included in the crystallization of the core complex (22). To analyze its structure, several positions were labeled. The corresponding EPR spectra exhibit sharp and narrowly spaced lines (Fig. 6) suggesting that those sites are unstructured. To compare the

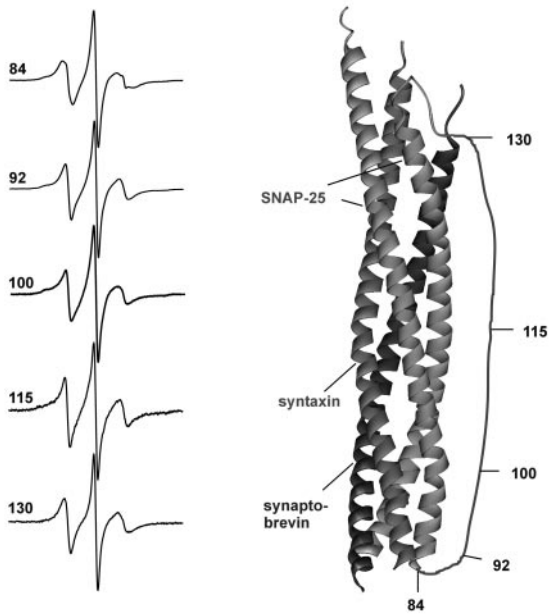

FIG. 6. **Structure of the loop region of SNAP-25 in the ternary complex as determined by EPR-spectroscopy.** The relative positions of the spin-labeled residues are indicated on the *right*. Note that the loop connecting the two SNAP-25 helices is drawn schematically, because it is not part of the crystal structure.

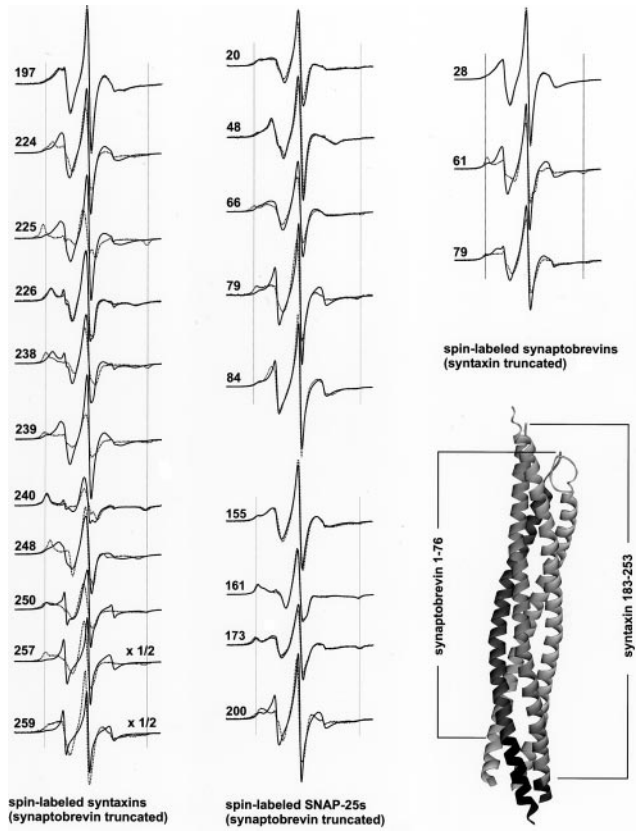

FIG. 7. **EPR spectra of ternary complexes containing truncated SNAREs.** Ternary complexes containing spin-labeled SNAREs were formed that contained either truncated synaptobrevin (residues 1–76) or syntaxin (residues 183–253) (see *scheme* at *bottom right*). For comparison, the corresponding spectra derived from the nontruncated complexes are indicated (*dotted lines*, data from Figs. 2 and 4). The amplitudes of spectra with sharp peaks (257 and 259) were multiplied by 1/2.

mobility at these sites with that of sites in the core complex (Fig. 2) we again determined the inverse second moment and the inverse of the central line width mobility parameters. As shown in Fig. 3, residues 84, 92, 100, 115, and 130 cluster in the region of highest mobility.

Core Complexes with Truncated SNAREs—We next investigated how C-terminal truncations of synaptobrevin and syntaxin affect the structure of the complex. Most importantly, we wanted to find out whether the perturbations of the complex structure caused by such a deletion remain local or whether they destabilize the complex in a more profound way. As outlined under "Discussion," a distinction between these possibilities is relevant for an understanding of the SNARE assembly and disassembly mechanism. As a starting point, we deleted residues that are also cleaved off by certain clostridial neurotoxins. The following mutants were generated: a syntaxin variant shortened by nine residues (residues 183–253, the latter corresponding to the cleavage site of botulinum neurotoxin/C), and a synaptobrevin variant shortened by 20 amino acids (residues 1–76, corresponding to the fragment generated by tetanus neurotoxin). With these mutants, sets of spin-labeled complexes were formed that were analyzed by EPR spectroscopy.

When the corresponding spectra of intact and truncated complexes were compared, several interesting features became apparent (Fig. 7). Unlike in the intact complex, no evidence for contact sites was found at C-terminal surface positions, suggesting that truncated complexes do not oligomerize. Immobile components in surface positions of syntaxin (*e.g.* positions 224, 225, and 239), synaptobrevin (positions 61 and 79), and a single position in SNAP-25 (position 66) largely disappeared and gave rise to typical helix surface spectra, similar to those of the N-terminal surface positions that remained unaltered. The monomeric state was confirmed by size-exclusion chromatography and multiangle laser light scattering (Table 1). Moreover, inwardly pointing residues (*e.g.* positions 226 and 240) located above the truncation site remained unaltered, documenting that the structure of the helical bundle is preserved N-terminal of the truncation site (Fig. 7). These data agree with other findings such as thermal stability and CD spectroscopy, which indicate that such truncations do not cause major overall changes in complex structure and stability.[2] Finally, labeling positions located in stretches of syntaxin and SNAP-25 that are C-terminal of the cleavage site in synaptobrevin yielded mobile spectra (Fig. 7), including residues 257 and 259 of syntaxin, residues 79 and 84 of SNAP-25 (N-terminal helix), and residue 200 of SNAP-25 (C-terminal helix). We conclude that the ends of the three helical segments collapse into random coils when the fourth partner is missing.

Binary Complex between Syntaxin and SNAP-25—In the last set of experiments, we investigated the structure of the binary complex formed by syntaxin and SNAP-25. Previous work has shown that in the absence of synaptobrevin these two proteins form a complex with a 2 (syntaxin):1 (SNAP-25) stoichiometry that is also α-helical but less stable than the ternary complex (29). Addition of synaptobrevin to such binary complexes results in the formation of ternary complexes, effectively displacing one of the syntaxin molecules. Because SNAP-25 and syntaxin are both localized in the plasma membrane, it is possible that such binary complexes form in the membrane and represent the physiological acceptor site for synaptobrevin upon vesicle docking.

Again, we generated sets of complexes containing labeled SNAP-25 and syntaxin variants. When the SNAP-25 spectra of the binary complexes were compared with those of the corresponding ternary complexes, most of the labeling positions were found to be nearly identical (Fig. 8*A*). These findings show

[2] M. Margittai, D. Fasshauer, S. Pabst, R. Jahn, and R. Langen, unpublished observations.

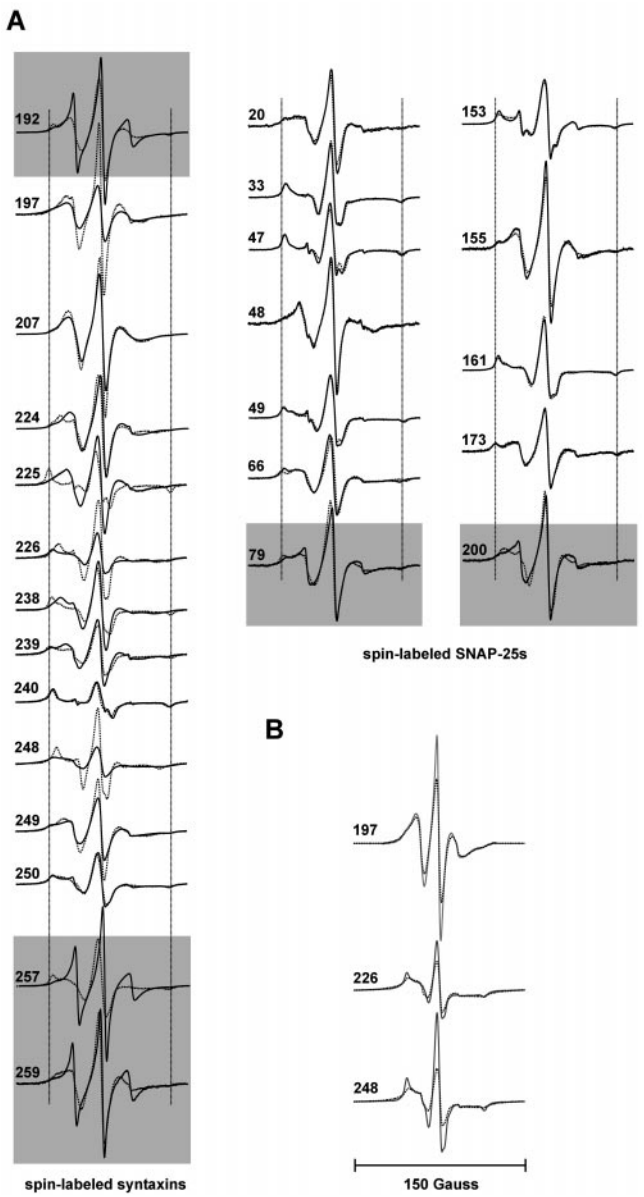

FIG. 8. **EPR spectra of binary complexes containing syntaxin and SNAP-25.** *A*, comparison of sets of spectra containing spin-labeled syntaxins or spin-labeled SNAP-25 variants. In each case, the binary complexes containing labeled variants were purified. For comparison, the corresponding spectra derived from the ternary complexes are indicated (*dotted lines*, data from Figs. 2 and 4). *Shaded areas* indicate spectra that are highly mobile in the binary complex. *B*, spin-spin coupling of syntaxin in the binary complex. Syntaxin variants spin labeled at positions 197, 226, and 248 were diluted with unlabeled syntaxin and combined with excess of SNAP-25 for complex formation. All spectra were recorded without further purification of the complexes. Spectra of complexes containing undiluted, labeled syntaxins are represented by *dotted lines*; spectra of complexes containing mixtures of labeled and unlabeled syntaxins are represented by *solid lines*. The scan width is 150 G.

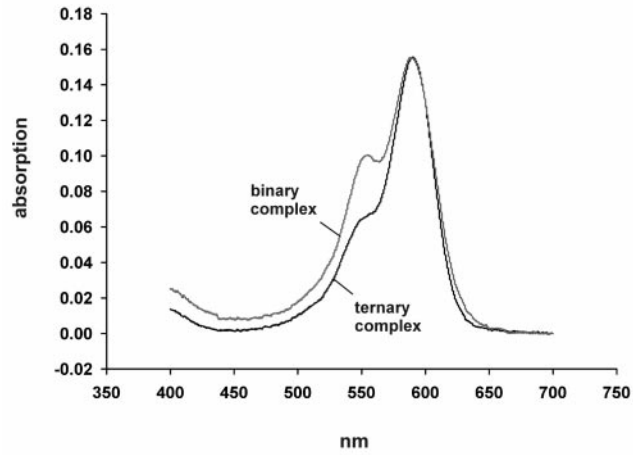

FIG. 9. **Absorption spectra of binary and ternary complexes (protein concentration 1.32 μM, containing syntaxin that is labeled at position 197 with Alexa594-maleimide.** Ternary complex was formed by addition of 10-fold molar excess of synaptobrevin.

that the structures of the two SNAP-25 helices closely resemble those of the ternary complex. The only significant differences are observed at the C-terminal ends of both helices (residues 79 and 200). Here the spectra indicate a higher degree of mobility. In contrast, the differences between the syntaxin spectra of the binary and ternary complexes were more profound. It should be borne in mind that the syntaxin spectra have contributions from two syntaxins and it is therefore not straightforward to assign the EPR spectra to individual syntaxins. Most importantly, labeling positions pointing inward in the complex are not only immobile but also show varying degrees of spin-spin coupling (residues 226 and 248) (Fig. 8*A*). Thus, residues pointing inward in the ternary complex also point inward in the binary complex, and because the corresponding amino acids are always close to each other, the two syntaxin helices must be oriented in parallel. With the exception of position 197, no spin-spin coupling was observed in labeling positions that do not point to the interior of the bundle. These observations were confirmed when increasing amounts of unlabeled syntaxin and SNAP-25 were added during complex formation (Fig. 8*B*). Spin-spin coupling disappeared whereas the overall character of the spectra remained unchanged.

To confirm the parallel alignment of the two syntaxins with an independent approach, we labeled position 197 of syntaxin with the dye Alexa594 (labeling efficiency >80%, data not shown). The absorption spectrum of binary complexes containing dye-labeled syntaxin showed a maximum at 590 nm and a second peak at 554 nm (Fig. 9). Addition of unlabeled synaptobrevin (Fig. 9) or of unlabeled syntaxin (not shown) resulted in a significant reduction of the maximum at 554 nm, yielding a spectrum very similar to the free dye. We conclude that the increased absorption at 554 nm is due to an interaction between adjacent chromophores that disappears upon displacement of one (or both) of the labeled syntaxins. The parallel alignment of both syntaxin molecules in the neuronal binary complex is compatible with the orientation needed for assembly in the plane of a membrane, in agreement with the notion that this complex may serve as an intermediate in SNARE assembly-disassembly pathways.

EPR spectra of surface positions in the C-terminal region were more similar (*i.e.* more mobile) to the truncated complex than to the intact ternary complex suggesting that the binary complex does not form oligomers. This conclusion was confirmed by size-exclusion chromatography and multiangle laser light scattering (Table 1). Finally, a high degree of mobility was found at the N- and C-terminal positions (residues 192 and 257–259). The latter corresponds to the higher mobility of the adjacent residues of SNAP-25, suggesting that the C-terminal end (corresponding to the region around layer 8 of the core complex) of the binary complex is unstructured. We conclude that the structure of the binary complex is similar to that of the ternary complex, representing an elongated and almost completely folded bundle of four α-helices in which one syntaxin molecule substitutes for synaptobrevin.

DISCUSSION

In the present study we have used site-directed spin labeling to study the structural features of SNARE proteins and SNARE complexes. Our data strengthen an emerging picture according to which SNARE proteins can switch back and forth between random and helical conformations and that such switching can either involve the entire SNARE motif or only parts of it in a highly adaptable manner.

Our data show that the monomers of both synaptobrevin 2 and SNAP-25 are unstructured over the entire length of their SNARE motifs. Such lack of secondary structure has already been deduced from CD spectroscopy (29, 30). Furthermore, our EPR data are in excellent agreement with the results of two-dimensional NMR spectroscopy (31). Similarly, the SNARE motif of syntaxin is also unstructured at low micromolar concentrations but oligomerizes into helical bundles with at least some of its helices arranged in parallel at higher concentrations. Self-association of this domain has been reported previously, but it remained unclear whether it forms defined oligomers or aggregates nonspecifically (19, 21, 25, 28).

A comparison of the EPR spectra of the monomers with those of the ternary complex highlight again the dramatic conformational changes the SNARE proteins undergo upon assembly into complexes. Such transitions appear to be essential features of all SNARE proteins as exemplified by the assembly of SNAREs operating in yeast exocytosis (45, 46) or in the fusion of late endosomes (47). In the fully assembled ternary complex, the structural predictions derived from the spectra of many different labeling positions are in excellent agreement with the previously determined crystal structure, which is represented by an elongated four-helix bundle. Furthermore, the EPR spectra confirm that the complex has a tendency to form oligomers.

The loop region connecting the two SNARE motifs of SNAP-25 is unstructured, explaining its sensitivity to protease digestion. Moreover, the high mobility of the side chains in the loop rules out significant contact between the loop and the surface of the helix bundle. It should be noted, however, that the loop region adjacent to the transmembrane domains contains four cysteines that are, at least in part, palmitoylated (residues 84, 85, 90, and 92) in the native protein. These palmitoyl side chains serve as membrane anchors and thus may induce structure in part of the loop.

Our data shed new light on the structure of the binary complex formed between SNAP-25 and syntaxin. Surprisingly, the complex is folded almost throughout its entire length, with only a few amino acid residues at the C- and N-terminal ends being unstructured. Because the spectra of almost all labeled SNAP-25 variants are superimposable between the binary and the ternary complex, the structures of the SNAP-25 helices must be largely identical. These properties differ substantially from the structural properties of the binary complex formed by the SNAREs functioning in yeast exocytosis (48). Here, the stoichiometry between Sec9p (corresponding to SNAP-25) and Sso1p (corresponding to syntaxin) is 1:1, suggesting that only three SNARE motifs are involved. NMR spectroscopy showed that in this complex Sso1p is helical only up to residue 240 with the C-terminal 24 residues remaining unstructured. Thus it is possible that the presence of an additional syntaxin in the neuronal binary complex is responsible for the extension of helical structure toward the C terminus. In the yeast complex, it is easy to imagine that the binary three-helix bundle forms a grooved acceptor site to which Sncp can bind. In contrast, in the neuronal binary complex the synaptobrevin binding site is occupied by the second syntaxin molecule. Because one of these syntaxins can easily be replaced by synaptobrevin, it is conceivable that one of the syntaxins is more loosely bound than the other.

The ternary complex containing truncated synaptobrevin appears to be perfectly intact upstream of the cleavage site, whereas the helices that face the stretch removed in the mutant become disordered at their C-terminal ends. Apparently, the formation of interacting layers in the core of the bundle is not dependent on the formation of layers in nearby positions. In other words, the findings support the view that SNARE complexes can assemble only partially in such a way that part of the helical bundle is correctly folded, whereas the remainder of all four participating SNARE motifs are unstructured. This feature agrees very well with the proposed "zippering" mechanism (8) and provides a structural basis for the hypothesis that defined complexes that are partially assembled form intermediates in the progression toward membrane fusion (33). These findings also support the emerging picture that the SNARE motifs are extremely versatile in their ability to undergo conformational changes. Apparently, SNARE motifs can switch between random coils and helical conformations in such a way that either the entire domain or only parts of the domain become α-helical with the rest remaining unstructured. These helices are characterized by the mostly hydrophobic ribbon of "layer" residues that have a tendency to interact with corresponding hydrophobic surfaces. The best evidence for such versatility is available for the SNARE motif of syntaxin. As shown in this study, this region can be unstructured (monomer at low concentrations), fully helical (core complex) (22), mostly helical except of the C- and N-terminal ends (homooligomer, binary complex) (this study), helical with a disordered C terminus (truncated complex (this study), full-length syntaxin in the "closed" conformation (28)), or composed of a consecutive helix-loop-helix structure with a disordered C-terminal end (in complex with Munc-18 (26)). Apparently, the length and position of the helix formed depends on the nature of the binding partners. Indeed, the capability of the SNARE motif to form molecular "velcro strips" of varying length may explain why syntaxin is capable to bind to many different proteins in an apparently specific manner.

Acknowledgments—We are greatly indebted to Maria Druminski for her superb help in plasmid construction and Wolfram Antonin for stimulating discussions and careful reading of the manuscript.

REFERENCES

1. Rothman, J. E. (1994) *Nature* **372,** 55–63
2. Jahn, R., and Südhof, T. C. (1999) *Annu. Rev. Biochem.* **68,** 863–911
3. Hughson, F. M. (1999) *Curr. Biol.* **9,** R49–R52
4. Brünger, A. T. (2000) *Curr. Opin. Neurobiol.* **10,** 293–302
5. Lin, R. C., and Scheller, R. H. (2000) *Annu. Rev. Cell Dev. Biol.* **16,** 19–49
6. Söllner, T., Whiteheart, S. W., Brunner, M., Erdjument-Bromage, H., Geromanos, S., Tempst, P., and Rothman, J. E. (1993) *Nature* **362,** 318–324
7. Söllner, T., Bennett, M. K., Whiteheart, S. W., Scheller, R. H., and Rothman, J. E. (1993) *Cell* **75,** 409–418
8. Hanson, P. I., Heuser, J. E., and Jahn, R. (1997) *Curr. Opin. Neurobiol.* **7,** 310–315
9. Terrian, D. M., and White, M. K. (1997) *Eur J. Cell Biol.* **73,** 198–204
10. Weimbs, T., Low, S. H., Chapin, S. J., Mostov, K. E., Bucher, P., and Hofmann, K. (1997) *Proc. Natl. Acad. Sci. U. S. A.* **94,** 3046–3051
11. Weimbs, T., Mostov, K., Low, S. H., and Hofmann, K. (1998) *Trends Cell Biol.* **8,** 260–262
12. Hayashi, T., McMahon, H., Yamasaki, S., Binz, T., Hata, Y., Südhof, T. C., and Niemann, H. (1994) *EMBO J.* **13,** 5051–5061
13. Pevsner, J., Hsu, S. C., Braun, J. E., Calakos, N., Ting, A. E., Bennett, M. K., and Scheller, R. H. (1994) *Neuron* **13,** 353–361
14. Hayashi, T., Yamasaki, S., Nauenburg, S., Binz, T., and Niemann, H. (1995) *EMBO J.* **14,** 2317–2325
15. Calakos, N., Bennett, M. K., Peterson, K. E., and Scheller, R. H. (1994) *Science* **263,** 1146–1149
16. Kee, Y., Lin, R. C., Hsu, S. C., and Scheller, R. H. (1995) *Neuron* **14,** 991–998
17. Chapman, E. R., An, S., Barton, N., and Jahn, R. (1994) *J. Biol. Chem.* **269,** 27427–27432
18. Zhong, P., Chen, Y. A., Tam, D., Chung, D., Scheller, R. H., and Miljanich, G. P. (1997) *Biochemistry* **36,** 4317–4326
19. Poirier, M. A., Hao, J. C., Malkus, P. N., Chan, C., Moore, M. F., King, D. S., and Bennett, M. K. (1998) *J. Biol. Chem.* **273,** 11370–11377
20. Hao, J. C., Salem, N., Peng, X. R., Kelly, R. B., and Bennett, M. K. (1997) *J. Neurosci.* **17,** 1596–1603
21. Fasshauer, D., Eliason, W. K., Brünger, A. T., and Jahn, R. (1998) *Biochemistry* **37,** 10354–10362

22. Sutton, R. B., Fasshauer, D., Jahn, R., and Brünger, A. T. (1998) *Nature* **395,** 347–353
23. Fasshauer, D., Sutton, R. B., Brünger, A. T., and Jahn, R. (1998) *Proc. Natl. Acad. Sci. U. S. A.* **95,** 15781–15786
24. Fernandez, I., Ubach, J., Dulubova, I., Zhang, X., Südhof, T. C., and Rizo, J. (1998) *Cell* **94,** 841–849
25. Lerman, J. C., Robblee, J., Fairman, R., and Hughson, F. M. (2000) *Biochemistry* **39,** 8470–8479
26. Misura, K. M., Scheller, R. H., and Weis, W. I. (2000) *Nature* **404,** 355–362
27. Hanson, P. I., Otto, H., Barton, N., and Jahn, R. (1995) *J. Biol. Chem.* **270,** 16955–16961
28. Dulubova, I., Sugita, S., Hill, S., Hosaka, M., Fernandez, I., Südhof, T. C., and Rizo, J. (1999) *EMBO J.* **18,** 4372–4382
29. Fasshauer, D., Otto, H., Eliason, W. K., Jahn, R., and Brünger, A. T. (1997) *J. Biol. Chem.* **272,** 28036–28041
30. Fasshauer, D., Bruns, D., Shen, B., Jahn, R., and Brünger, A. T. (1997) *J. Biol. Chem.* **272,** 4582–4590
31. Hazzard, J., Südhof, T. C., and Rizo, J. (1999) *J. Biomol. NMR* **14,** 203–207
32. Hanson, M. A., and Stevens, R. C. (2000) *Nat. Struct. Biol.* **7,** 687–692
33. Xu, T., Rammner, B., Margittai, M., Artalejo, A. R., Neher, E., and Jahn, R. (1999) *Cell* **99,** 713–722
34. Hubbell, W. L., Cafiso, D. S., and Altenbach, C. (2000) *Nat. Struct. Biol.* **7,** 735–739
35. Hubbell, W. L., McHaourab, H. S., Altenbach, C., and Lietzow, M. A. (1996) *Structure* **4,** 779–783
36. Hubbell, W. L., Gross, A., Langen, R., and Lietzow, M. A. (1998) *Curr. Opin. Struct. Biol.* **8,** 649–656
37. Feix, J. B., and Klug, C. S. (1998) in *Biological Magnetic Resonance Vol. 14, Spin Labeling: The Next Millenium* (Berliner, L. J., ed) pp. 251–281, Plenum Press, New York
38. McHaourab, H. S., Lietzow, M. A., Hideg, K., and Hubbell, W. L. (1996) *Biochemistry* **35,** 7692–7704
39. Langen, R., Oh, K. J., Cascio, D., and Hubbell, W. L. (2000) *Biochemistry* **39,** 8396–8405
40. Rabenstein, M. D., and Shin, Y. K. (1995) *Proc. Natl. Acad. Sci. U. S. A.* **92,** 8239–8243
41. Farrens, D. L., Altenbach, C., Yang, K., Hubbell, W. L., and Khorana, H. G. (1996) *Science* **274,** 768–770
42. Poirier, M. A., Xiao, W., Macosko, J. C., Chan, C., Shin, Y. K., and Bennett, M. K. (1998) *Nat. Struct. Biol.* **5,** 765–769
43. Fasshauer, D., Antonin, W., Margittai, M., Pabst, S., and Jahn, R. (1999) *J. Biol. Chem.* **274,** 15440–15446
44. Higuchi, R. (1990) in *PCR Protocols: A Guide to Methods and Applications* (Innis, M. A., Gelfand, D. H., Sinisky, J. J., and White, T. J., eds) pp. 177–183, Academic Press, New York
45. Rice, L. M., Brennwald, P., and Brünger, A. T. (1997) *FEBS Lett.* **415,** 49–55
46. Nicholson, K. L., Munson, M., Miller, R. B., Filip, T. J., Fairman, R., and Hughson, F. M. (1998) *Nat. Struct. Biol.* **5,** 793–802
47. Antonin, W., Holroyd, C., Fasshauer, D., Pabst, S., Fischer von Mollard, G., and Jahn, R. (2000) *EMBO J.* **19,** 6453–6464
48. Fiebig, K. M., Rice, L. M., Pollock, E., and Brünger, A. T. (1999) *Nat. Struct. Biol.* **6,** 117–123

PROTEIN STRUCTURE AND FOLDING:

Homo- and Heterooligomeric SNARE Complexes Studied by Site-directed Spin Labeling

Martin Margittai, Dirk Fasshauer, Stefan Pabst, Reinhard Jahn and Ralf Langen

J. Biol. Chem. 2001, 276:13169-13177.
doi: 10.1074/jbc.M010653200 originally published online January 19, 2001